Structure and dynamics of room temperature ionic liquids with bromide anion: Results from 81Br NMR spectroscopy

doi: 10.1002/mrc.4208

Structure and Dynamics of Room Temperature Ionic Liquids with Bromide Anion: Results from ^{81}Br NMR Spectroscopy

Takatsugu Endo,*[,†] Mamoru Imanari,[‡] Yuki Hidaka,[§] Hiroko Seki,[‡] Keiko Nishikawa,[§] and Sabyasachi Sen[‖]

[†]*Graduate School of Natural Science and Technology, Kanazawa University, Kakuma-machi, Kanazawa-shi, Ishikawa 920-1192, Japan*

[‡]*Center for Analytical Instrumentation, Chiba University, 1-33 Yayoi-cho, Inage-ku, Chiba-shi, Chiba 263-8522, Japan*

[§]*Graduate School of Advanced Integration Science, Chiba University, 1-33 Yayoi-cho, Inage-ku, Chiba-shi, Chiba 263-8522, Japan*

[‖]*Department of Chemical Engineering and Materials Science, The University of California, Davis, One Shield Avenue, Davis, California 95616, USA*

Abstract

We report the results of a comprehensive ^{81}Br NMR spectroscopic study of the structure and dynamics of two RTILs, 1-butyl-3-methylimidazolium bromide ([C_4mim]Br) and 1-butyl-2,3-dimethylimidazolium bromide ([C_4C_1mim]Br), in both liquid and crystalline states. NMR parameters in the gas phase are also simulated for stable ion pairs using quantum chemical calculations. The combination of ^{81}Br spin-lattice and spin-spin relaxation measurements in the motionally narrowed region of the stable liquid state provides information on the correlation time of the translational motion of the cation. ^{81}Br quadrupolar coupling constants (C_Q) of the two RTILs is estimated to be 6.22 MHz and 6.52 MHz in the crystalline state which reduce by nearly 50% in the liquid state although in the gas phase the values are higher and span the range of 7 to 53 MHz depending on ion pair structure. The C_Q can be correlated with the distance between the cation-anion pairs in all the three states. The ^{81}Br C_Q values of the bromide anion in the liquid state indicate the presence of some structural order in these RTILs, the degree of which decreases with increasing temperature. On the other hand, the iconicity of these RTILs is estimated from the combined knowledge of the isotropic chemical shift and the appropriate mean energy of the excited state. [C_4C_1mim]Br has higher ionicity than [C_4mim]Br in the gas phase while the situation is reverse for the liquid and the crystalline states.

1. Introduction

Room temperature ionic liquids (RTILs) are salts that are liquid around ambient temperature. As liquids, these materials are characterized by outstanding properties including extremely low vapor pressure, negligible flammability and high thermal/electrochemical/chemical stability that may enable their potential applications as electrolytes, chemical reaction media, extraction solvents and catalysts, to name a few. [1–5] A fundamental understanding of the molecular structure and its control on the transport properties are therefore essential for the development of predictive models of the behavior of these materials relevant to these wide ranging applications.

Halide ions, i.e. chloride, bromide and iodide, are typical constituent anions for RTILs although it may be noted that monoatomic F^- anions are not available for RTILs in general.[4,6] The small size of the halide monoatomic anions tends to result in relatively high melting temperature and viscosity of RTILs. However, such simple anions are advantageous as model systems for experimental studies as they facilitate the analyses and interpretation of experimental data for RTILs. Nuclear magnetic resonance (NMR) spectroscopy is one of the most effective experimental methods to obtain exclusive and element-specific information of the structure and dynamics of a wide range of RTILs. Specifically, all the halogen nuclides : ^{35}Cl/^{37}Cl, ^{79}Br/^{81}Br and ^{127}I are detectable with NMR but only a few studies have been reported on halogen NMR in neat RTILs especially on bromides and iodides.[7–9] Recently, Gordon et al. reported NMR spectra and parameters of these quadrupole nuclides using various cations paired with halide anions that form RTILs.[8] Nevertheless, detailed discussion on NMR parameters and the dynamical behavior of halide anions in RTILs remain lacking partly because NMR spectroscopy of these nuclides are rather challenging owing to their low sensitivity and large quadrupole moments that result in broad and complicated line shapes. Here we report the results of a ^{81}Br NMR spectroscopic study of the structure and dynamics of two RTILs with Br^- (bromide) anions: 1-butyl-3-methylimidazolium bromide ([C_4mim]Br) and 1-butyl-2,3-dimethylimidazolium bromide ([C_4C_1mim]Br) (Chart 1), in both the crystalline and liquid states as well as calculations in the gas phase, modeled by ion pairs. The objective of this

study is to reveal what structural and dynamical information ^{81}Br NMR spectra give for RTILs with bromide anion. Isotropic chemical shift (δ_{iso}) and quadrupole coupling constant (C_Q) are derived and discussed in this paper for all the three states in addition to correlation time in the liquid state. One of the focus of this study is on the effect of the methylation at the 2 position of the imidazolium cation rings since the methylation strongly influences a number of properties in these RTILs,[10–16] including melting point and viscosity, that are somewhat counterintuitive

2. Experimental

The details of the synthesis of [C_4mim]Br and [C_4C_1mim]Br are described elsewhere.[11] They are prepared from 1-methylimidazole or 1,2-dimethylimidazole mixed with a slight excess 1-bromobutane. The samples were dried at ca. 333 K under vacuum (10^{-3} Pa) for over 24 h before use. All sample handling was performed in N_2 atmosphere in a glove box to avoid absorption of atmospheric moisture. These procedures reduced the water content of the sample typically below 100 ppm.[12] The samples were characterized by ^{1}H NMR.

Single-pulse ^{81}Br NMR spectra of the two samples in the liquid state were collected using a JEOL JNM-ECX400 spectrometer equipped with a 9.4 T magnet (^{81}Br Larmor frequency = 107.97 MHz), and a JEOL JNM-ECA600 spectrometer equipped with a 14.0 T magnet for the solid state (^{81}Br Larmor frequency = 162.09 MHz). All ^{81}Br chemical shifts were externally referenced to either 0.01 M NaBr-D_2O solution (δ_{iso} = 0 ppm) or crystalline KBr powder (δ_{iso} = 54.51 ppm[17]). Temperature was calibrated using methanol and glycerin[18–21] for the data collected at the lower field and using $Pb(NO_3)_2$[22,23] for the data collected at the higher field. The samples for the liquid state measurements were sealed in a 4-mm NMR tube under vacuum, and then the sealed tube was inserted into a 5-mm NMR tube. Deuterium solvents were placed in the gap between 4-mm and 5-mm NMR tubes for deuterium locking if necessary. The ^{81}Br NMR spectra were collected with a recycle delay of 0.1 s and 8192 free induction decays (FID) were averaged and Fourier-transformed to

obtain each spectrum. The ^{81}Br NMR spin-lattice relaxation times (T_1) were measured using the saturation recovery method while spin-spin relaxation times (T_2) were estimated from the linewidth. The length of the 90º saturation pulses for the T_1 experiments was set to be 17.0 μs - 17.5 μs. This pulse length was long enough to possibly allow for partial relaxation especially for the low temperature region where T_1 could be on the order of ~ 50 μs. However, in all cases the time dependence of the recovered magnetization was well fitted with a single exponential with an appropriate offset. For measurements in the solid state, crushed powder samples were taken in a 4-mm zirconia rotor and spun at 10 to 20 kHz. The ^{81}Br magic-angle-spinning (MAS) NMR (Bloch decay) spectra were collected with a recycle delay of 0.5 s and 2048 free induction decays (FID) were averaged and Fourier-transformed to obtain each spectrum. The pulse length of 2.3 μs was used. The ^{81}Br MAS NMR line shapes were simulated using the Dmfit program.[24]

3. DFT Modeling of gas phase

Full geometry optimization analyses for the cation-anion pairs in the gas phase as well as the other computations were carried out using density functional theory (DFT) within the Gaussian 09 program package.[25] The 6-311+G(d,p) basis sets based on Becke's three-parameter hybrid method[26] with the LYP correlation (B3LYP) were used.[27,28] No imaginary frequencies were produced by the optimized structures; this ensured the presence of a minimum. The corresponding ^{81}Br NMR parameters were computed using the continuous set of gauge transformations (CSGT) method.[29–31] Natural bond orbital (NBO) analyses were conducted to obtain negative charge on the bromide anion using the B3LYP/6-311+G(d,p) as well as the Møller-Plesset second-order perturbation theory (MP2)[32] with aug-cc-pVDZ[33] basis sets. The chemical shift of a central Br atom in a cubic KBr cluster ($K_{14}Br_{13}$) was used as a reference (σ_{iso} = 2697.2 ppm and δ_{iso} = 54.51 ppm). The supermolecular method was used to calculate the interaction energy between a cation and an anion, which was corrected for the basis set superposition error.

4. Results

Crystalline state

The structures of [C_4mim]Br and [C_4C_1mim]Br crystals obtained from single-crystal X-ray refinement were already reported by Holbrey et al.[34] and Kutuniva et al.,[35] respectively. The bromide anion occupies a single site in both crystal structures. In the case of the [C_4mim]Br structure, the closest approach between a cation and the Br^- anion is the hydrogen atom at the 2 position of the imidazolium ring (see Chart 1). The corresponding H···Br distance between the ions is 2.450 Å. On the other hand, in the [C_4C_1mim]Br crystal, the hydrogen at the 4 position in the cation is the closest one to the Br^- anion with an H···Br distance of 2.733 Å. These differences in the relative positions of the cation-anion pairs in these two RTILs are believed to be responsible for the different effects of the methylation on their properties. The methylation prohibits the interaction between the anion and the proton at the 2 position, which causes lower interaction energy as predicted by previous quantum chemical calculations.[10]

The solid-state ^{81}Br MAS NMR spectra of the two RTILs obtained with two different spinning speeds are shown in Figure 1. The experimental line shapes are typical of central transition line shapes of quadrupolar nuclides and can be simulated well using a single set of quadrupolar parameters corresponding to a single Br site in each compound. The corresponding isotropic chemical shift δ_{iso}, quadrupole coupling constant C_Q and electric field gradient tensor asymmetry parameter (η) are summarized in Table 1. These parameters for [C_4mim]Br compare well with those reported in a previous study by Gordon et al.[8] It should be noted that they reported on ^{79}Br, and C_Q ($=eQq_{xx}/h$, where e is the charge of an electron, Q is the quadrupole moment, q_{zz} is the largest principal component of electric field gradient tensor, h is the Planck's constant) depends on quadrupole moment Q. Considering quadrupole moment ratio of ^{79}Br to ^{81}Br, our data gives 7.44 MHz as ^{79}Br C_Q, which is close to the previous value of 7.35 MHz. ^{81}Br NMR parameters for the RTIL [C_4C_1mim]Br are similar but distinguishable from those characteristic of [C_4mim]Br (Table

1). The C_Q values increase by the presence of the methyl group at the 2 position of the imidazolium ring, which was also seen in chloride-based RTIL system.[36] This may be a characteristic feature for the methylation effect. These RTILs have relatively large ^{81}Br δ_{iso} and small C_Q values compared to those reported in the literature for other organic salts including RTILs.[8,37,38]

Liquid state

Figure 2 shows the temperature dependence of the static (non-spinning) ^{81}Br NMR spectra for both RTILs in the liquid state, including the supercooled liquid region. The corresponding variation in the spectral peak position and full width at half maximum (FWHM) are displayed in Figure 3. Both quantities display a pronounced nonlinear variation with temperature with maxima near ~345 K for [C_4mim]Br and near ~380 K for [C_4C_1mim]Br. It should be pointed out that these temperatures are similar to the melting points of these RTILs: 353 K and 369.8 K, respectively, for [C_4mim]Br and [C_4C_1mim]Br.[11] Such maxima in the temperature dependence of the peak position and FWHM are often typical of quadrupolar nuclides and results from the motional averaging of the quadrupolar interaction.[39] In the low temperature region where the quadrupolar nuclide under observation does not have enough mobility, the apparent chemical shift of the central transition is shifted upfield from the isotropic position by the second order quadrupolar interaction. Increasing rotational and translational mobility of the nuclide with increasing temperature would result in averaging of the second order quadrupolar interaction and the apparent chemical shift will move progressively downfield to ultimately coincide with the isotropic shift as the quadrupolar shift becomes negligible. Further increase in temperature will result in variation in the isotropic chemical shift from changes of local environment and/or thermal expansion effects, and this crossover may be manifested in a discontinuity in slope or a local maximum in the chemical shift as a function of temperature as seen in Figure 3.

In the case of a quadrupolar nuclide such as ^{81}Br with $I = 3/2$, the satellite transition peaks (i.e., −3/2 to −1/2 and +1/2 to +3/2) are too broad to observe directly along with the

central transition. However, these satellite peaks move in and eventually merge with the central transition thereby increasing the apparent FWHM of the central peak with progressive motional averaging of the quadrupolar interaction. In the high temperature regime above ~345 K and 380 K for [C_4mim]Br and [C_4C_1mim]Br, respectively, the quadrupolar interaction is fully averaged and the normal temperature induced line narrowing behavior typical of non-quadrupolar (I= ½) nuclides returns. In this region the FWHM of the ^{81}Br NMR spectra of these RTILs is controlled by the spin-spin relaxation time T_2. The FWHM of [C_4mim]Br is always smaller than that of [C_4C_1mim]Br, which indicates that the latter RTIL has lower mobility of the Br^- ions, consistent with its higher viscosity compared to that of [C_4mim]Br, which would be caused by the methylation.[13,15,16]

The T_1 and T_2 data (Figure 4) for the two RTILs in the liquid state are required to derive C_Q. T_2 were estimated from FWHM,

$$\frac{1}{T_2} = \pi FWHM \qquad (1)$$

T_1 and T_2 in the motionally narrowed regime can be expressed as: [40,41]

$$\frac{1}{T_1} = \frac{3\pi^2}{200}\frac{2I+3}{I^2(2I-1)}\left(1+\frac{\eta^2}{3}\right)C_Q^2\left(2J(\omega)+8J(2\omega)\right) \qquad (2)$$

$$\frac{1}{T_2} = \frac{3\pi^2}{200}\frac{2I+3}{I^2(2I-1)}\left(1+\frac{\eta^2}{3}\right)C_Q^2\left(3J(0)+5J(\omega)+2J(2\omega)\right) \qquad (3)$$

$$J(\omega) = \frac{2\tau_{Br}}{1+(\omega\tau_{Br})^2} \qquad (4)$$

where I is the spin quantum number, ω is the resonance (Larmor) frequency of ^{81}Br, τ_{Br} is the correlation time for the fluctuation of the C_Q of ^{81}Br nuclides resulting from dynamics in the RTIL. τ_{Br} can be obtained from Eq. 5,

$$\frac{T_2}{T_1} = \frac{2J(\omega)+8J(2\omega)}{3J(0)+5J(\omega)+2J(2\omega)} \qquad (5)$$

The τ_{Br} values thus obtained are plotted as a function of temperature in Figure 5 (a). The slower ionic dynamics in [C_4C_1mim]Br is evident from its τ_{Br} values that are longer than

those obtained for [C_4mim]Br, consistent with the FWHM data as mentioned above (Figure 3 (b)). Once τ_{Br} values are determined, C_Q can be obtained from Eq. 2, and the result is shown in Figure 5 (b). Although the η values are not known in the liquid state, they hardly affect the values of C_Q, then it was assumed to be zero in the state.

Gas phase modeled as ion pair

RTILs were considered to be non-volatile materials for long time. In 2006, it was revealed that they could be distilled at a certain pressure and temperature.[42] Although their structure in the gas phase is still controversial, a neutral cation-anion pair can be regarded as the main component.[43–46] The NMR parameters of stable ion pairs in the gas phase were obtained with DFT calculations. There are some likely combinations of several anion interaction sites with different cation conformations as shown in Figure 6. Based on the previous studies in the literature on the ion pairs of the RTILs containing the same ions,[10,47,48] the numbers of considered anion sites and cation conformations were set to be 7 and 3, respectively, that means, 21 different pairs were considered. The two anion sites are placed above (TOP) and beneath (BOTTOM) the imidazolium ring, and the others are coplanar to the ring, such as the ones between the proton at the 2 position (H2) and the methyl group (front-methyl, FM), H2 and the butyl group (front-butyl, FB), the protons at the 4 (H4) and 5 (H5) positions (BACK), H4 and the methyl group (side-methyl, SM), and H5 and the butyl group (side-butyl, SB). These abbreviation were taken from the paper by Hunt.[10] Three cation conformations are expressed as gauche-trans (GT), trans-trans (TT) and gauche'-trans (G'T).

The calculated energy differences, interaction energy between the cation and anion (ΔE_{int}) as well as the population of the ion pairs are summarized in Table 2. The most stable ion pair structure is FB-TT for [C_4mim]Br and TOP-TT for [C_4C_1mim]Br. Their populations roughly account for one fourth to one third of the total. The Gibbs free energy difference ΔG (from the most stable conformer) of the ion pairs classified SB and SM are significantly high, then their populations are negligible although they exist as the stable ion pairs. ΔE_{int} in [C_4mim]Br seems to be larger than those in [C_4C_1mim]Br. In order to

compare the interaction energies directly, the population-weighted average energies were derived at standard temperature and pressure, which are −357.6 kJ mol^{-1} for [C_4mim]Br and −342.1 kJ mol^{-1} for [C_4C_1mim]Br. The higher interaction energy of [C_4mim]Br compared to that of [C_4C_1mim]Br is similar to the observation made in a previous study for the corresponding chloride salts with the same cation.[10] This similarity corroborates with the hypothesis that the C2 methylation reduces the cation-anion interaction energy as indicated by Hunt for the chloride analogues.[10]

The numbers of the stable anion interaction sites are 16 and 13 for [C_4mim]Br and [C_4C_1mim]Br, respectively. Entropy for each ion pair set can be derived using the following equation,

$$S = -R\sum_i \rho_i \ln\rho_i \qquad (6)$$

where R is the gas constant and ρ_i is the fractional population of each ion pair state i. The calculated entropies of [C_4mim]Br and [C_4C_1mim]Br at 298.15 K and 1 atm are 15.7 J K^{-1} mol^{-1} and 13.1 J K^{-1} mol^{-1}, respectively, which again confirms Hunt's hypothesis on the basis of her study of [C_4mim]Cl and [C_4C_1mim]Cl[10] that the entropic change by the methylation provides a partial explanation for the counterintuitive increase of melting point and viscosity.

The calculations of the ^{81}Br NMR parameters for these stable ion pairs were performed and the results are listed in Table 3. The NMR parameters drastically depend on not only the anion site but also the cation conformation. To make comparison between the two RTILs in a simple way, population-weighted average values at 298.15 K were again used (Table 3 bottom). Large difference is observed in δ_{iso} between the RTILs, e.g. 140.2 ppm for [C_4mim]Br and −71.3 ppm for [C_4C_1mim]Br. The difference in C_Q, 15.57 MHz for [C_4mim]Br and 22.59 MHz for [C_4C_1mim]Br, is modest compared to chemical shift, but still significant.

5. Discussion

Dynamics in the liquid state

First, we clarify the origin of the ion motion that defines the τ_{Br} obtained from the T_1 and T_2 data. The correlation times are based on the fluctuation of electrical field gradient at the sites of the Br^- anions. This fluctuation can be attributed to the translational motions of the anion and/or the cation as well as to the rotational or reorientational motions of the cations. Although translational motion of the Br anions have not been reported for these RTILs, previous pulsed field gradient (PFG) and ^{13}C T_1 NMR studies revealed translational and reorientational motions for the cation of $[C_4mim]Br$, respectively.[12,49] Figure 7 shows a comparison between the τ_{Br} obtained in this study and the reported correlation times for translational (τ_{trans}) and ring reorientational (τ_{reori}) motion of the $[C_4mim]^+$ cation in $[C_4mim]Br$. The τ_{trans} values are obtained from diffusion coefficient D_{trans} measured by PFG NMR[49] using the relation:[41]

$$\tau_{trans} = \frac{d^2}{2D_{trans}} \qquad (7)$$

where d is the distance of the closest approach. The value d can be defined as $d = 2a$ where a is the radius of a molecule when the molecule is assumed to be a sphere. Molecular volume of $[C_4mim]^+$ was reported to be 150 $Å^3$,[50] thereby a is estimated to be 3.30 Å. It is clear from Figure 7 that τ_{Br} is an order of magnitude slower than τ_{reori} but is almost the same as τ_{trans}. It is known that anion translations in imidazolium-based RTILs are somewhat slower than that of cations.[51–53] In this scenario, τ_{Br} primarily represents the fluctuation of the electric field gradient at the Br sites due to the translational motion of the cations in the liquid state. Since viscosity of RTILs is generally so high that measurements of the diffusion coefficients of ions need special NMR probe. The method adopted here to obtain τ_{Br} is feasible with a conventional NMR setup by measuring T_1 and T_2. Only T_1 experiments are practically necessary because T_2 can be estimated from linewidth.

NMR parameters in three states

The ^{81}Br δ_{iso} and C_Q have been obtained in all the three states. The simulated values of the ion pairs in the gas phase show larger difference between [C_4mim]Br and [C_4C_1mim]Br than in the other two states. [C_4mim]Br has larger δ_{iso} values in all the states than [C_4C_1mim]Br does, while the opposite is true for the C_Q. Since these NMR parameters reflect electrical environment of the Br anions, it is suggested that the consistency of the parameters in the three states originates from the methylation. However, the values in the liquid state show temperature dependence and comparison at same temperature would not be appropriate because larger C_Q can remain in more viscous environment. Comparing at same viscosity would be a more proper way to discuss the methylation effect. Unfortunately, there seems to be not reliable viscosity data for these RTILs, therefore we use τ_{Br} instead, as shown in Figure 8. While the gap in chemical shift becomes more significant, the trend is reversed in C_Q. In the following sections, these parameters are discussed in detail separately.

Quadrupole coupling constant C_Q

While C_Q of [C_4C_1mim]Br is larger than that of [C_4mim]Br in the crystalline state and the gas phase, the opposite is true in the liquid state in terms of viscosity dependence. We start the discussion with the situation in the gas phase. C_Q reflects magnitude of electric field gradient, and the former increases with increasing the latter. As was previously observed in n-alkyltrimethylammonium bromide,[37] the distance between a cation and an anion can govern C_Q. Figure 9 shows C_Q versus $r_{c\text{-}a}$ where $r_{c\text{-}a}$ is the distance between the anion and the closet carbon or nitrogen atom in the cation ring. The C_Q values for both RTILs are well correlated with the distance $r_{c\text{-}a}$. The $r_{c\text{-}a}$ values are rather larger in [C_4C_1mim]Br than [C_4mim]Br, which would be the result of the methylation effect.

However, this idea seems not to be applicable in the crystalline state. The distance $r_{c\text{-}a}$ in [C_4mim]Br and [C_4C_1mim]Br in the state were estimated to be 3.514 Å and 3.653 Å, respectively,[34,35] although C_Q is larger in [C_4C_1mim]Br (Table 1). If we extrapolate C_Q values for the crystals from Figure 9 using the $r_{c\text{-}a}$ values, C_Q in the range of 5 to 8 MHz is

assessed, which are comparable to those in the crystalline state. This finding implies that the correlation between C_Q and $r_{c\text{-}a}$ is essentially correct, nevertheless, the error bar is large enough to allow some exceptions. The existence of multiple inter-ion interactions between the cations and anions in the crystalline state beyond nearest neighbors is important to consider when comparing to the gas phase where the relationship of the cation and anion is 1 to 1.

In the liquid state, although C_Q of $[C_4C_1mim]Br$ looks larger than that of $[C_4mim]Br$ at the same temperature (Figure 5 (b)), the former becomes slightly smaller or almost the same as the latter when the same τ_{Br} is compared (Figure 8 (b)). The previous X-ray diffraction and MD simulation indicated that there would be no significant change of the cation-anion distance in the imidazolium-based RTILs by the methylation.[14] It is likely that the data in the literature were taken at room temperature, thereby the methylated RTIL would show the subtly longer ion distance at the same τ_{Br} due to thermal expansion. This is in line with the C_Q data obtained here.

It should be noted that the fact that the both RTILs possess non-zero C_Q values for ^{81}Br (approximately half of that in the crystalline state) indicates there is a certain structure in the liquid state, contradictory to the suggestion in the previous report on ^{79}Br NMR measurements for RTILs.[8] The Br anions do not show any C_Q if their electric field is completely spherical. This finding is reminiscent of the concept of "local structure in RTILs".[54,55] It is known that RTILs in the liquid state still keep a similar structure to that in the crystalline state. Temperature increase causes C_Q to decrease, which indicates that the Br anion loses specific interactions with the cation in high temperature region, and possesses more spherical electrical environment. The C_Q of halide anions in the liquid state of RTILs could be a measure of the magnitude of the structuring.

Isotropic Chemical shift δ_{iso}

As was already mentioned above, the δ_{iso} of $[C_4mim]Br$ is larger than that of $[C_4C_1mim]Br$ in all the three state. Comparing experimentally obtained values for the liquid and crystalline states, although the former is smaller than the latter, the difference by the

methylation is almost the same as 10 ppm. Again, we start the discussion from δ_{iso} in the gas phase. δ_{iso} of some halide anions were reported to depend on the cation-anion distance.[37,38,56,57] However, the RTILs studied here do not show any relationship with the distance (Figure S1). On the other hand, δ_{iso} shows a rough correlation with negative charge of the bromide anion (or ionicity) that is estimated with NBO calculations at B3LYP/6-311+G(d,p) level (Figure 10 (a), Pearson's r = 0.558). The correlation becomes better when the higher calculation level of MP2/aug-cc-pVDZ is employed (Pearson's r = 0.650). δ_{iso} is expressed as the difference of magnetic shielding (σ) between a target sample and a reference,

$$\delta_{iso} = \sigma_{ref} - \sigma_{sample} \qquad (8)$$

and σ_{sample} is,

$$\sigma_{sample} = \sigma_d + \sigma_p \qquad (9)$$

where σ_d (positive in sign) and σ_p (negative in sign) are diamagnetic and paramagnetic terms, respectively. The paramagnetic contribution of ionic crystals is known to depend on the cation-anion overlap in σ_p term,[37,56–58] which could be related to the cation-anion distance. More precisely, σ_p is,[59,60]

$$\sigma_p = -\frac{8}{3} z\lambda\mu_B \frac{1}{\Delta E_m}\left\langle \frac{1}{r^3} \right\rangle_p \qquad (10)$$

where z is the coordination number, λ is the degree of covalency, that is, $(1 - \lambda)$ is the ionicity, μ_B is the Bohr magneton, ΔE_m is the mean energy of the excited state and $\langle 1/r^3 \rangle_p$ is the mean of $1/r^3$ of the valence p-electron. Since σ_d for ^{13}C is almost constant in general, δ_{iso} can be proportional to ionicity. The ionicity was derived from Eq. 10 with $\langle 1/r^3 \rangle_p$ = 13.55,[61] and shown in Figure 10 (b). ΔE_m values were assessed by time-dependent (TD) DFT calculations (see Table S1 and its caption for details), which are estimated to be 3.411 eV and 3.667 eV for $[C_4mim]Br$ and $[C_4C_1mim]Br$, respectively. A good correlation is observed between the negative charges from NBO and the δ_{iso} values with Eq. 10 (Pearson's r = 0.865). It should be noted that Pearson's r becomes 0.936 if one outlier is removed. The linearity demonstrates that the classical theoretical equation enables the

estimation of the ionicity for RTILs. Some deviation in the correlation is still observed because several assumptions were employed, such as r is independent on the RTILs and ΔE_m values were taken from the DFT calculations in the gas phase. Uncertainty of the NMR parameters and NBO calculations with the levels also contributes to the diversity. However, considering the lack of sophisticated treatments, the linearity would be satisfactory. It is demonstrated that the ionicity for RTILs can be estimated from δ_{iso} with aid of the DFT calculations.

This idea was applied into the both liquid and crystalline states. Figure 11 shows the temperature dependence of the negative charge in the liquid state estimated with Eq. 10. Temperature increase results in the increase of negative charge (or ionicity) for both RTILs. This would be caused by lowered cation-anion interactions due to higher ion mobility and thermal expansion, which destroys structures in the liquid state and brings the charge on the ions closer to their formal values. [C_4C_1mim]Br shows slightly smaller ionicity than [C_4mim]Br. This is also true in the crystalline state because the δ_{iso} difference is almost the same. Those of [C_4mim]Br and [C_4C_1mim]Br were estimated to be −0.857 and −0.849, respectively. Ionicity of the liquid state seems to be higher than that of the crystalline state. This result can be explained by the volume expansion by melting. The majority of materials including RTILs[62,63] expands their volume 10 to 15 % by melting, which results in increasing cation-anion distance and thereby increases ionicity of the anions. The trend of the ionicity is reversed compared to the gas phase. The results rely somewhat on the ΔE_m values that are not obtained experimentally, therefore detailed discussion must be conducted with caution. However, considering the facts that C_Q and $r_{c\text{-}a}$ are also not consistent in the three states, the ionicity in the liquid and crystalline states can be opposite to the gas phase.

Ionicity is an important property for RTILs. Although there are several approaches proposed to estimate this parameter ever, using Walden plot seems to be the main stream.[64–66] Here we propose that δ_{iso} of bromide ions in RTILs with calculated ΔE_m values can be a good indicator to assess ionicity. It should be pointed out that this method should be applicable for other halide anions, that is, chloride and iodide.

6. Conclusion

We have performed ^{81}Br NMR spectroscopy for two RTILs, [C_4mim]Br and [C_4C_1mim]Br in their liquid and crystalline states. Quantum chemical calculations of the NMR parameters are performed on the ion pairs in the gas phase. T_1 and T_2 measurements in the narrowing region of the liquid provide the correlation time τ_{Br} as well as C_Q. It is revealed that τ_{Br} represents the translational motion of the cation, but could include the anion translational motion as well. The C_Q values of [C_4mim]Br and [C_4C_1mim]Br in the crystalline state are estimated to be around 6.22 MHz and 6.52 MHz, respectively, and reduce by half in the liquid state and decrease with increasing temperature. In the ion pair model the values can be correlated to the distance between the cation and anion, and this is also applicable in the liquid and crystalline states. [C_4mim]Br has higher isotropic chemical shift than [C_4C_1mim]Br in all the three states. The classical theoretical treatment of paramagnetic shielding (Eq. 10) implies that the difference in the δ_{iso} of the Br anion originates mainly from the ionicity of the anion and therefore, can be a good indicator of ionicity.

We have confirmed that ^{81}Br NMR spectroscopy is a useful tool to investigate structure and dynamics of RTILs containing Br anions. The methylation effect at the 2 position of the imidazolium ring explicitly appears in the differences between the ^{81}Br NMR parameters. Although there are already a few papers reporting on RTILs with ^{79}Br/^{81}Br NMR spectroscopy which gives intriguing aspects of the ions,[7–9] it should be emphasized that our comprehensive data set covering crystalline, liquid and gas states provides profound insights of the bromide anion at the molecular level, such as quadrupole coupling constant and ionicity in all the states as well as correlation time that represents translation motion in the liquid state.

Acknowledgements

The present study was supported by the Ministry of Education, Culture, Sports, Science and Technology of Japan No. 21245003 Grant-in-Aid for Scientific Research (A) and the Global Center-of-Excellence Program "Advanced School for Organic Electronics" as well as a JSPS Postdoctoral Fellowships for Research Abroad to T. Endo.

References

[1] *Topics in Current Chemistry*; Kirchner, B., Ed.; Springer-Verlag Berlin: Berlin, Germany, 2009.

[2] I. Minami, *Molecules* **2009**, *14*, 2286.

[3] *Ionic Liquids: Applications and Perspectives*; Kokorin, A., Ed.; InTech, 2011.

[4] P. Wasserscheid, T. Welton, *Ionic Liquids in Synthesis*; VCH-Wiley: Weinheim, Germany, 2003.

[5] H. Ohno, *Electrochemical Aspects of Ionic Liquids*; Wiley-Interscience: Hoboken, 2005.

[6] E. A. Turner, C. C. Pye, R. D. Singer, *J. Phys. Chem. A* **2003**, *107*, 2277.

[7] V. Balevicius, Z. Gdaniec, K. Aidas, J. Tamuliene, *J. Phys. Chem. A* **2010**, *114*, 5365.

[8] P. G. Gordon, D. H. Brouwer, J. A. Ripmeester, *ChemPhysChem* **2010**, *11*, 260.

[9] V. Klimavicius, Z. Gdaniec, V. Balevicius, *Spectrochim. Acta Part A Mol. Biomol. Spectrosc.* **2014**, *132*, 879.

[10] P. A. Hunt, *J. Phys. Chem. B* **2007**, *111*, 4844.

[11] T. Endo, T. Kato, K. Nishikawa, *J. Phys. Chem. B* **2010**, *114*, 9201.

[12] T. Endo, M. Imanari, H. Seki, K. Nishikawa, *J. Phys. Chem. A* **2011**, *115*, 2999.

[13] K. Fumino, A. Wulf, R. Ludwig, *Angew. Chemie - Int. Ed.* **2008**, *47*, 8731.

[14] K. Fujii, T. Mitsugi, T. Takamuku, T. Yamaguchi, Y. Umebayashi, S. Ishiguro, *Chem. Lett.* **2009**, *38*, 340.

[15] K. Noack, P. S. Schulz, N. Paape, J. Kiefer, P. Wasserscheid, A. Leipertz, *Phys. Chem. Chem. Phys.* **2010**, *12*, 14153.

[16] E. I. Izgorodina, R. Maganti, V. Armel, P. M. Dean, J. M. Pringle, K. R. Seddon, D. R. MacFarlane, *J. Phys. Chem. B* **2011**, *115*, 14688.

[17] R. P. Chapman, C. M. Widdifield, D. L. Bryce, *Prog. Nucl. Magn. Reson. Spectrosc.* **2009**, *55*, 215.

[18] A. L. Van Geet, *Anal. Chem.* **1968**, *40*, 2227.

[19] A. L. Van Geet, *Anal. Chem.* **1970**, *42*, 679.

[20] D. S. Raiford, C. L. Fisk, E. D. Becker, *Anal. Chem.* **1979**, *51*, 2050.

[21] C. Ammann, P. Meier, A. Merbach, *J. Magn. Reson.* **1982**, *46*, 319.

[22] A. Bielecki, D. P. Burum, *J. Magn. Reson. Ser. A* **1995**, *116*, 215.

[23] T. Takahashi, H. Kawashima, H. Sugisawa, T. Baba, *Solid State Nucl. Magn. Reson.* **1999**, *15*, 119.

[24] D. Massiot, F. Fayon, M. Capron, I. King, S. Le Calvé, B. Alonso, J.-O. Durand, B. Bujoli, Z. Gan, G. Hoatson, *Magn. Reson. Chem.* **2002**, *40*, 70.

[25] M. J. Frisch, G. W. Trucks, H. B. Schlegel, G. E. Scuseria, M. A. Robb, J. R. Cheeseman, G. Scalmani, V. Barone, B. Mennucci, G. A. Petersson, H. Nakatsuji, M. Caricato, X. Li, H. P. Hratchian, A. F. Izmaylov, J. Bloino, G. Zheng, J. L. Sonnenberg, M. Hada, M. Ehara, K. Toyota, R. Fukuda, J. Hasegawa, M. Ishida, T. Nakajima, Y. Honda, O. Kitao, H. Nakai, T. Vreven, J. A. Montgomery Jr., J. E. Peralta, F. Ogliaro, M. Bearpark, J. J. Heyd, E. Brothers, K. N. Kudin, V. N. Staroverov, T. Keith, R. Kobayashi, J. Normand, K. Raghavachari, A. Rendell, J. C. Burant, S. S. Iyengar, J. Tomasi, M. Cossi, N. Rega, J. M. Millam, M. Klene, J. E. Knox, J. B. Cross, V. Bakken, C. Adamo, J. Jaramillo, R. Gomperts, R. E. Stratmann, O. Yazyev, A. J. Austin, R. Cammi, C. Pomelli, J. W. Ochterski, R. L. Martin, K. Morokuma, V. G. Zakrzewski, G. A. Voth, P. Salvador, J. J. Dannenberg, S. Dapprich, A. D. Daniels, O. Farkas, J. B. Foresman, J. V. Ortiz, J. Cioslowski, D. J. Fox, Gaussian 09 **2010**.

[26] A. D. Becke, *J. Chem. Phys.* **1993**, *98*, 5648.

[27] C. Lee, W. Yang, R. G. Parr, *Phys. Rev. B* **1988**, *37*, 785.

[28] B. Miehlich, A. Savin, H. Stoll, H. Preuss, *Chem. Phys. Lett.* **1989**, *157*, 200.

[29] T. A. Keith, R. F. W. Bader, *Chem. Phys. Lett.* **1992**, *194*, 1.

[30] T. A. Keith, R. F. W. Bader, *Chem. Phys. Lett.* **1993**, *210*, 223.

[31] J. R. Cheeseman, *J. Chem. Phys.* **1996**, *104*, 5497.

[32] C. Møller, M. S. Plesset, *Phys. Rev.* **1934**, *46*, 618.

[33] R. A. Kendall, T. H. Dunning, R. J. Harrison, *J. Chem. Phys.* **1992**, *96*.

[34] J. D. Holbrey, W. M. Reichert, M. Nieuwenhuyzen, S. Johnston, K. R. Seddon, R. D. Rogers, *Chem. Commun.* **2003**, 1636.

[35] J. Kutuniva, R. Oilunkaniemi, *Z. Naturforsch. B* **2007**, *62b*, 868.

[36] P. G. Gordon, D. H. Brouwer, J. a Ripmeester, *J. Phys. Chem. A* **2008**, *112*, 12527.

[37] B. Alonso, D. Massiot, P. Florian, H. H. Paradies, P. Gaveau, T. Mineva, *J. Phys. Chem. B* **2009**, *113*, 11906.

[38] K. M. N. Burgess, I. Korobkov, D. L. Bryce, *Chem. - A Eur. J.* **2012**, *18*, 5748.

[39] A. M. George, J. F. Stebbins, *Phys. Chem. Miner.* **1996**, *23*, 526.

[40] B. Halle, H. Wennerström, *J. Magn. Reson.* **1981**, *44*, 89.

[41] A. Abragam, *Principles of Nuclear Magnetism*; Oxford University Press: Oxford, 1961.

[42] M. J. Earle, J. M. S. S. Esperança, M. A. Gilea, J. N. C. Lopes, L. P. N. Rebelo, J. W. Magee, K. R. Seddon, J. A. Widegren, *Nature* **2006**, *439*, 831.

[43] J. P. Armstrong, C. Hurst, R. G. Jones, P. Licence, K. R. J. Lovelock, C. J. Satterley, I. J. Villar-Garcia, *Phys. Chem. Chem. Phys.* **2007**, *9*, 982.

[44] J. P. Leal, J. M. S. S. Esperança, M. E. M. da Piedade, J. N. C. Lopes, L. P. N. Rebelo, K. R. Seddon, *J. Phys. Chem. A* **2007**, *111*, 6176.

[45] V. V Chaban, O. V Prezhdo, *J. Phys. Chem. Lett.* **2012**, *3*, 16571662.

[46] D. Strasser, F. Goulay, M. S. Kelkar, E. J. Maginn, S. R. Leone, *J. Phys. Chem. A* **2007**, *111*, 3191.

[47] S. Tsuzuki, R. Katoh, M. Mikami, *Mol. Phys.* **2008**, *106*, 1621.

[48] S. Tsuzuki, A. A. Arai, K. Nishikawa, *J. Phys. Chem. B* **2008**, *112*, 7739.

[49] M. Kohagen, M. Brehm, Y. Lingscheid, R. Giernoth, J. Sangoro, F. Kremer, S. Naumov, C. Iacob, J. Kärger, R. Valiullin, B. Kirchner, *J. Phys. Chem. B* **2011**, *115*, 15280.

[50] H. Machida, R. Taguchi, Y. Sato, R. L. Smith, *Fluid Phase Equilib.* **2009**, *281*, 127.

[51] H. Tokuda, K. Hayamizu, K. Ishii, M. A. B. H. Susan, M. Watanabe, *J. Phys. Chem. B* **2004**, *108*, 16593.

[52] H. Tokuda, K. Hayamizu, K. Ishii, M. A. B. H. Susan, M. Watanabe, *J. Phys. Chem. B* **2005**, *109*, 6103.

[53] H. Tokuda, K. Ishii, M. A. B. H. Susan, S. Tsuzuki, K. Hayamizu, M. Watanabe, *J. Phys. Chem. B* **2006**, *110*, 2833.

[54] K. Iwata, H. Okajima, S. Saha, H. Hamaguchi, *Acc. Chem. Res.* **2007**, *40*, 1174.

[55] C. Chiappe, *Monatsh. Chem.* **2007**, *138*, 1035.

[56] H. Trill, H. Eckert, V. I. Srdanov, *J. Phys. Chem. B* **2003**, *107*, 8779.

[57] D. L. Bryce, G. D. Sward, *Magn. Reson. Chem.* **2006**, *44*, 409.

[58] J. Kondo, J. Yamashita, *J. Phys. Chem. Solids* **1959**, *10*, 245.

[59] A. Saika, C. P. Slichter, *J. Chem. Phys.* **1954**, *22*, 26.

[60] K. Yosida, T. Moriya, *J. Phys. Soc. Japan* **1956**, *11*, 33.

[61] R. G. Barnes, W. V Smith, *Phys. Rev.* **1954**, *93*, 95.

[62] J. Yang, X. Lu, J. Gui, W. Xu, *Green Chem.* **2004**, *6*, 541.

[63] J. Dupont, P. A. Z. Suarez, *Phys. Chem. Chem. Phys.* **2006**, *8*, 2441.

[64] P. Ingman, G. W. Driver, *Phys. Chem. Chem. Phys.* **2012**, *14*, 13053.

[65] K. Ueno, H. Tokuda, M. Watanabe, *Phys. Chem. Chem. Phys.* **2010**, *12*, 1649.

[66] D. R. MacFarlane, M. Forsyth, E. I. Izgorodina, A. P. Abbott, G. Annat, K. Fraser, *Phys. Chem. Chem. Phys.* **2009**, *11*, 4962.

Supporting Information

Additional supporting information may be found in the online version of this article at the publisher's website.

Table 1. ^{81}Br NMR parameters of the two RTILs in the crystalline state. MAS experiments with four different speeds (10, 15, 18 and 20 kHz) were performed, and the mean values are displayed.

	[C_4mim]Br	[C_4C_1mim]Br
δ_{iso} / ppm	174.6 ± 1.8	163.5 ± 1.3
C_Q / MHz	6.22 ± 0.07	6.52 ± 0.19
η	0.87 ± 0.0	0.57 ± 0.0

Table 2. Energy and Gibbs free energy differences (ΔE and ΔG), population of ion pairs (at 298.15 K and 1 atm) and interaction energy (ΔE_{int}) in the gas phase calculated with the DFT method.

		[C_4mim]Br				[C_4C_1mim]Br			
		ΔE	ΔG	Population	ΔE_{int}	ΔE	ΔG	Population	ΔE_{int}
TOP	GT	n/a				0.00	0.00	0.343	–344.0
	TT	0.66	2.83	0.088	–357.6	0.36	0.26	0.309	–343.5
	G'T	n/a				5.47	5.36	0.040	–338.3
BOTTOM	GT	2.85	7.49	0.013	–355.3	2.93	4.43	0.057	–340.3
	TT	1.70	6.76	0.018	–356.3	2.09	3.18	0.095	–341.3
	G'T	5.06	8.84	0.008	–353.0	5.49	1.96	0.156	–338.0
FM	GT	0.00	1.79	0.135	–358.5	n/a			

	TT	0.20	0.25	0.250	–358.3	n/a			
	G' T	1.15	2.81	0.089	-357.2	n/a			
FB	GT	4.11	3.99	0.055	-354.4	n/a			
	TT	0.46	0.00	0.276	–358.0	n/a			
	G' T	1.46	3.52	0.067	–357.0	n/a			
SM	GT	35.03	37.83	< 0.001	–323.5	27.58	23.34	< 0.001	–316.7
	TT	33.34	34.68	< 0.001	–325.2	26.16	18.95	< 0.001	–318.1
	G' T	33.33	36.04	< 0.001	–325.3	27.74	23.26	< 0.001	–316.5
SB	GT	32.75	35.52	< 0.001	–325.7	26.66	23.15	< 0.001	–317.6
	TT	29.48	31.89	< 0.001	–328.9	23.60	17.12	< 0.001	–320.5
	G' T	33.14	36.07	< 0.001	–325.4	29.21	22.52	< 0.001	–315.1
BACK	GT	n/a				n/a			
	TT	n/a				51.99	37.38	< 0.001	–292.4
	G' T	n/a				n/a			

Table 3. Calculated ^{81}Br NMR parameters for the ion pairs in the gas phase.

		[C_4mim]Br			[C_4C_1mim]Br		
		δ_{iso}	C_Q	η	δ_{iso}	C_Q	η
TOP	GT	n/a			−111.8	8.41	0.47
	TT	156.6	32.97	0.12	−21.4	25.60	0.53
	G'T	n/a			−73.3	15.29	0.52
BOTTOM	GT	51.5	52.38	0.18	−77.4	34.59	0.57
	TT	19.3	51.46	0.18	−74.6	33.26	0.57
	G'T	104.7	47.15	0.17	−94.6	32.60	0.51
FM	GT	133.2	11.74	0.59	n/a		
	TT	162.1	12.49	0.67	n/a		
	G'T	149.0	10.41	0.87	n/a		
FB	GT	125.1	12.06	0.95	n/a		
	TT	135.8	11.29	0.55	n/a		
	G'T	152.1	11.69	0.70	n/a		
SM	GT	55.2	10.27	0.07	64.6	8.28	0.28
	TT	69.8	10.26	0.15	71.3	8.10	0.37
	G'T	61.3	10.25	0.06	67.3	8.17	0.20
SB	GT	89.1	9.09	0.53	66.2	8.61	0.36
	TT	25.0	9.23	0.54	17.9	7.76	0.56
	G'T	20.5	11.14	0.36	−4.3	11.13	0.30
BACK	GT	n/a			n/a		
	TT	n/a			−11.5	13.01	0.63
	G'T	n/a			n/a		

population weighted average		140.2	15.57	0.58	−71.3	22.59	0.52

Chart 1. Structure of [C_4mim]Br and [C_4C_1mim]Br

FIGURE CAPTIONS

Figure 1. ^{81}Br NMR spectra of [C_4mim]Br (black) and [C_4C_1mim]Br (red) in the crystalline state at room temperature. Pale lines (gray and pink) are the simulation result using Dmfit program. (a) 10 kHz (b) 15 kHz

Figure 2. Temperature dependence of ^{81}Br NMR spectra in the liquid state including supercooled liquid region. (a) [C_4mim]Br: 303.6 K to 415.8 K. (b) [C_4C_1mim]Br: 341.6 K to 415.8 K.

Figure 3. (a) Isotropic chemical shift (δ_{iso}) and (b) FWHM of [C_4mim]Br (black) and [C_4C_1mim]Br (red) in the liquid state against temperature estimated from Figure 2.

Figure 4. T_1 (filled circles) and T_2 (open circles) plots for [C_4mim]Br (black) and [C_4C_1mim]Br (red)

Figure 5. (a) Correlation time τ_{Br} and (b) C_Q of [C_4mim]Br (black) and [C_4C_1mim]Br (red) in the liquid state

Figure 6. Calculated ion pair structures. FM: front-methyl, FB: front-butyl, SM: side-methyl, SB: side-butyl, GT: gauche-trans (−60º), TT: trans-trans (180º), G'T: gauche'-trans (60º).

Figure 7. Various correlation times for $[C_4mim]^+$ paired with Br^- against temperature. Correlation times for the cation translation (τ_{trans}, blue symbols),[49] cation ring reorientation (τ_{reori}, green line)[12] and the Br anion obtained here (τ_{Br}, black symbols).

Figure 8. (a) Chemical shift and (b) C_Q in the liquid state versus the correlation time τ_{Br} for [C_4mim]Br (black) and [C_4C_1mim]Br (red).

Figure 9. Calculated C_Q of [C_4mim]Br (black) and [C_4C_1mim]Br (red) versus $r_{c\text{-}a}$ for the ion pairs in the gas phase where $r_{c\text{-}a}$ is the distance between the anion and the closet carbon or nitrogen atom in the cation ring.

Figure 10. (a) Negative charge of the Br anion in the ion pairs of the RTILs calculated with NBO analyses (red: B3LYP/6-311+G(d,p), blue: MP2/aug-cc-pVDZ) versus chemical shift and (b) the relationship between negative charges estimated with NBO analysis with the MP2 level and using Eq. 10 for [C_4mim]Br (black) and [C_4C_1mim]Br (red) in the gas phase. Blue line is the linear fit.

Figure 11. Negative charge of the Br anion in the liquid state of [C_4mim]Br (black) and [C_4C_1mim]Br (red) against (a) temperature and (b) τ_{Br}.

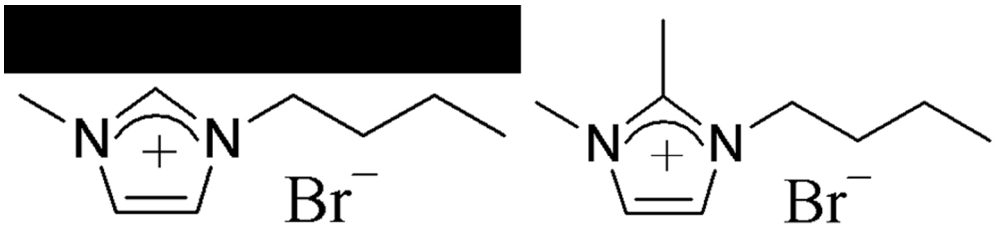

170x38mm (150 x 150 DPI)

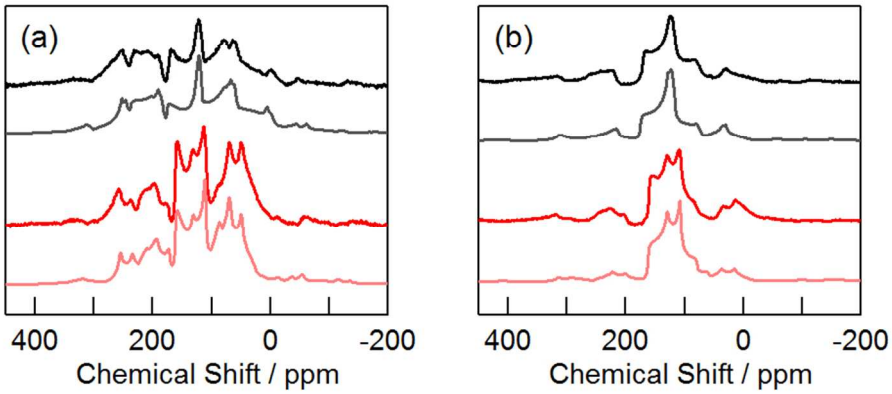

173x78mm (150 x 150 DPI)

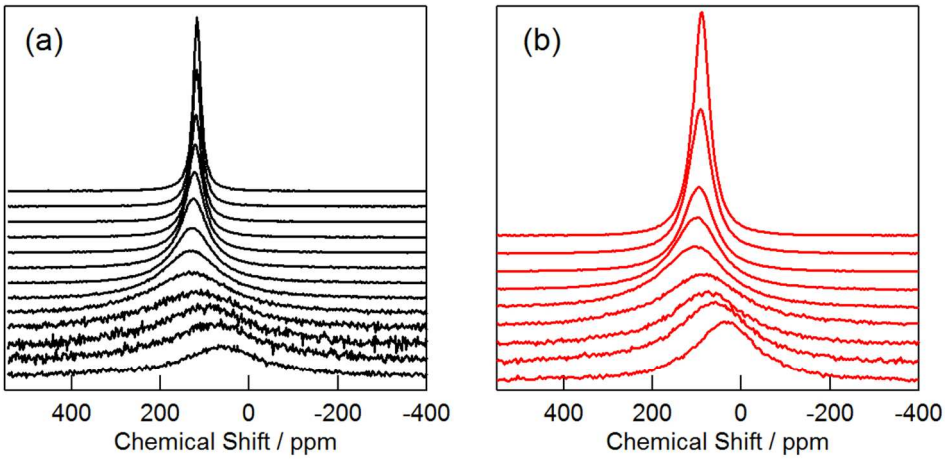

205x104mm (150 x 150 DPI)

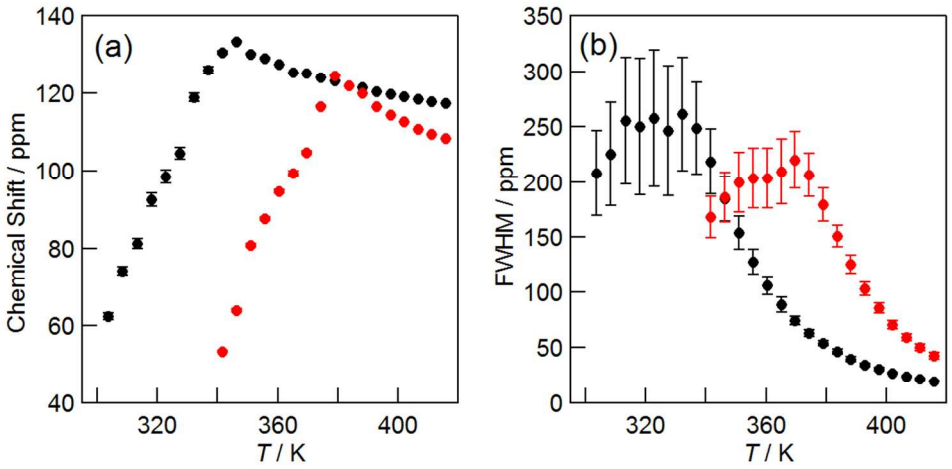

203x104mm (150 x 150 DPI)

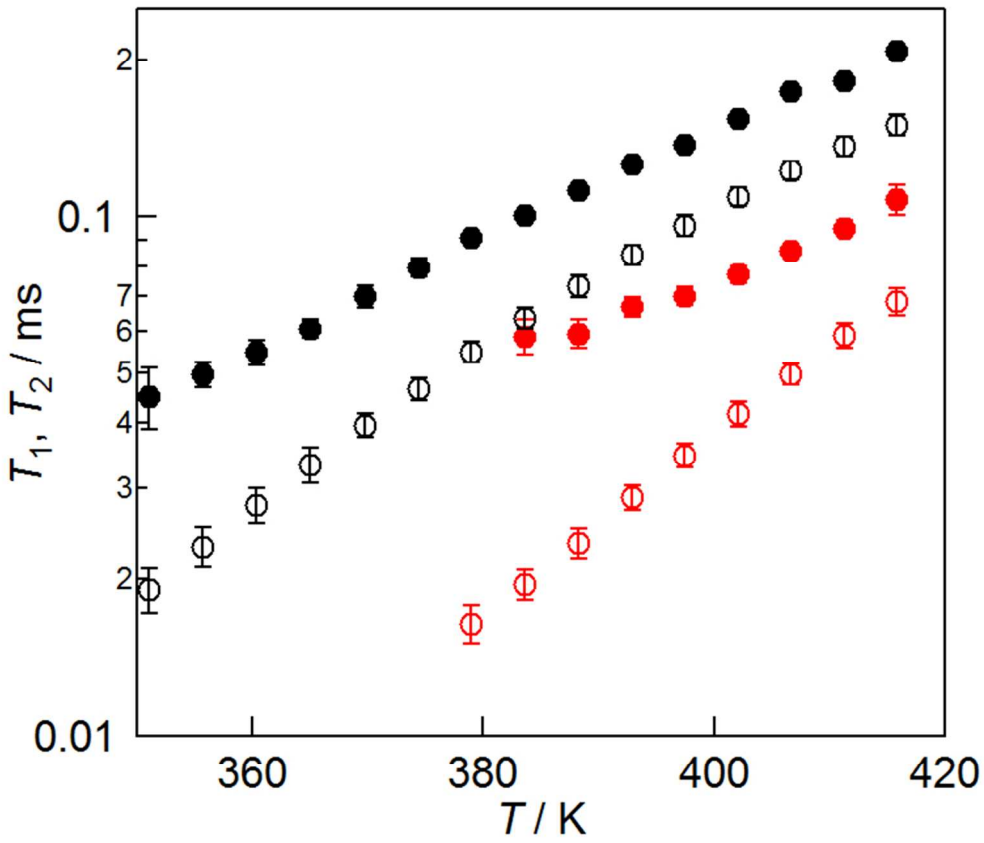

129x117mm (150 x 150 DPI)

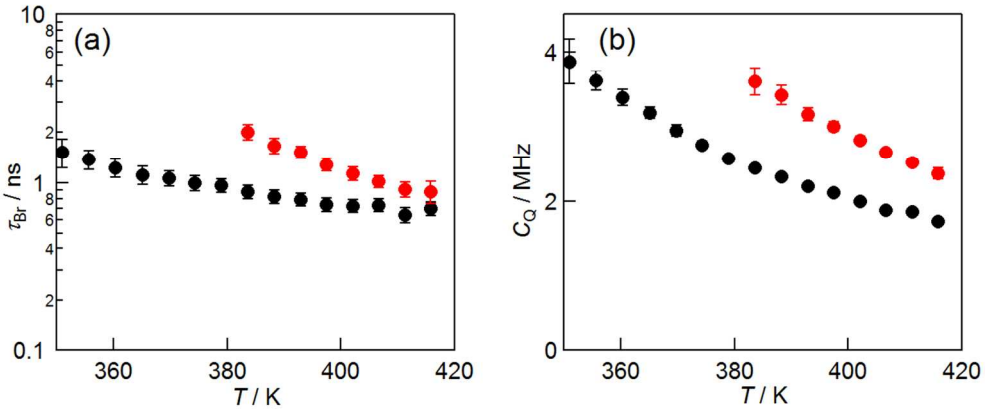

211x91mm (150 x 150 DPI)

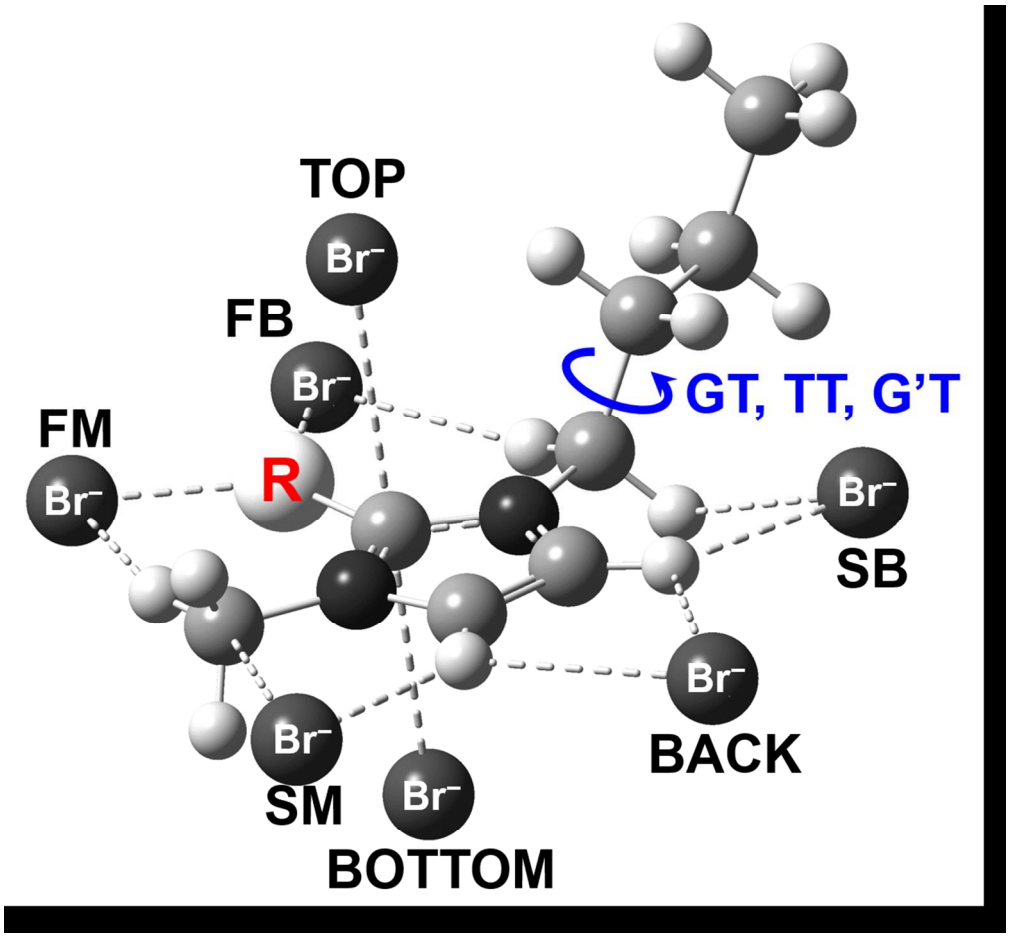

211x196mm (150 x 150 DPI)

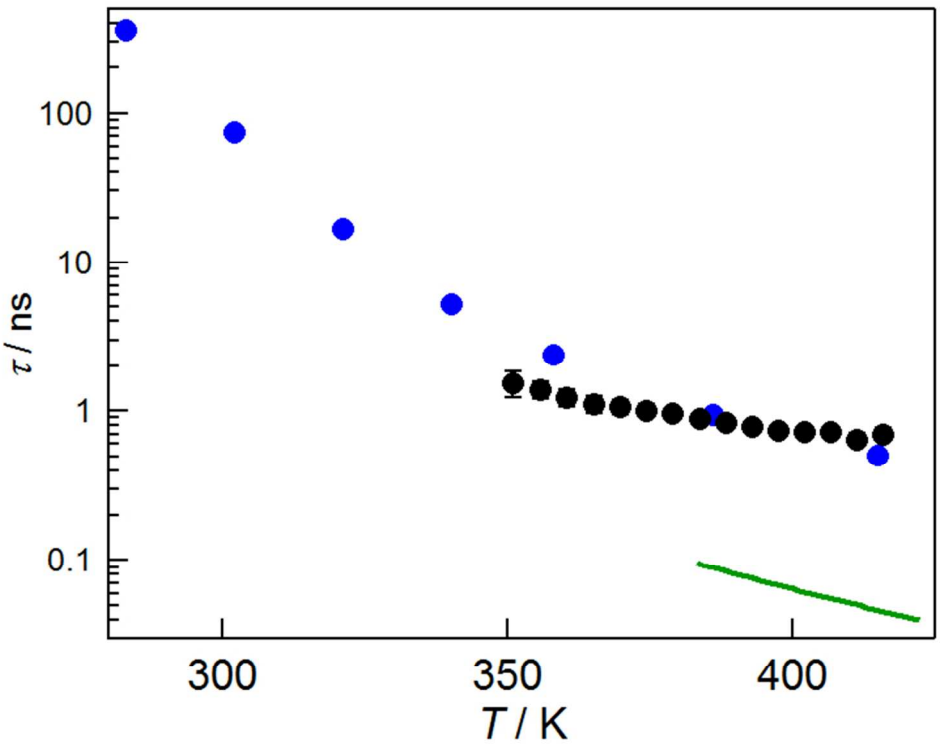

129x104mm (150 x 150 DPI)

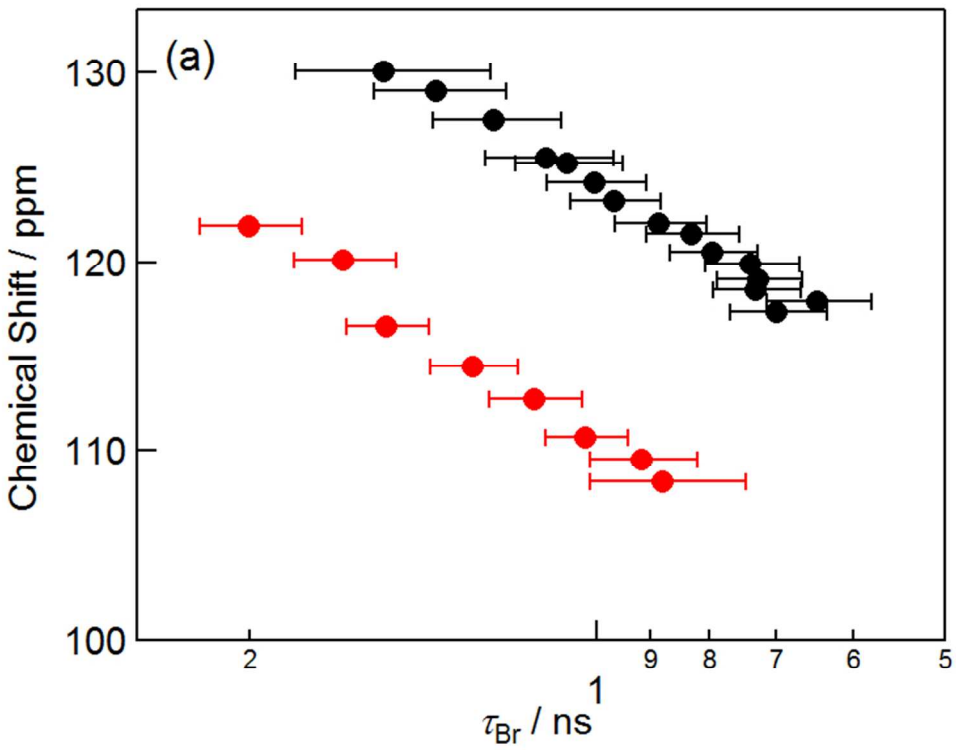

129x104mm (150 x 150 DPI)

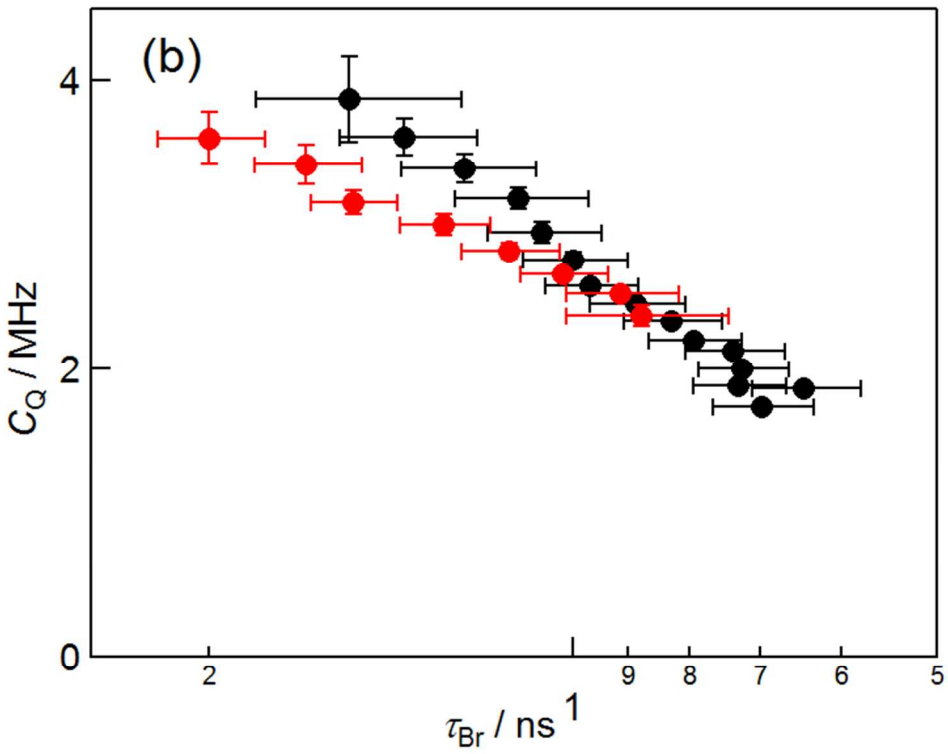

129x104mm (150 x 150 DPI)

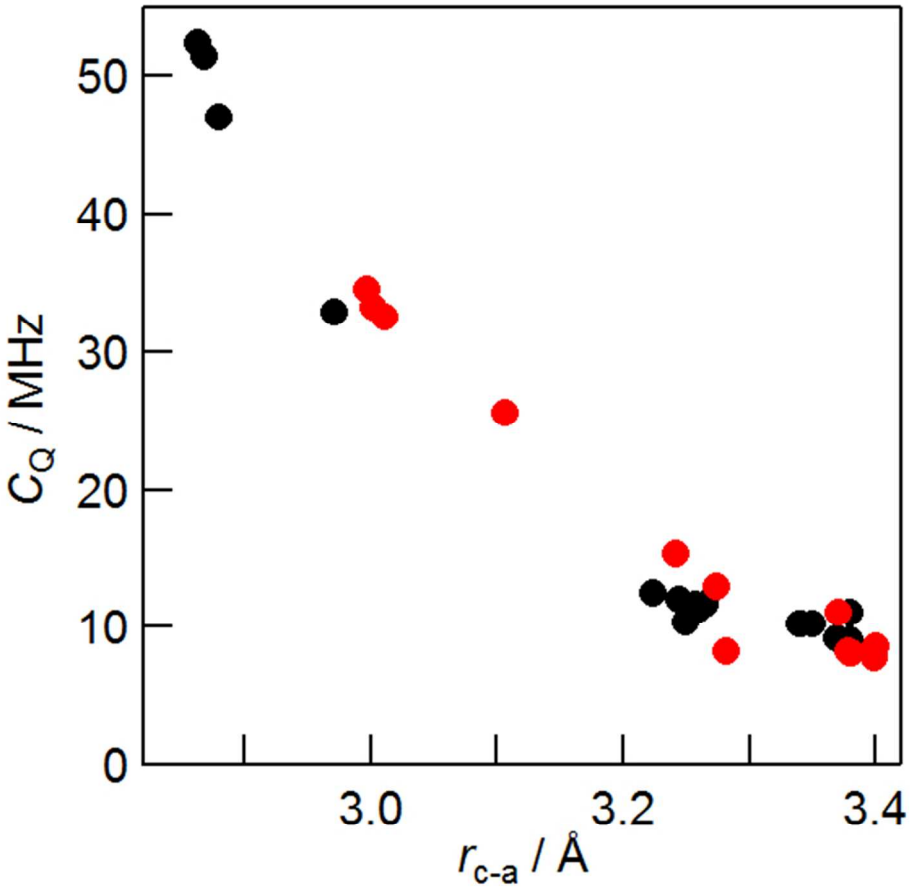

104x104mm (150 x 150 DPI)

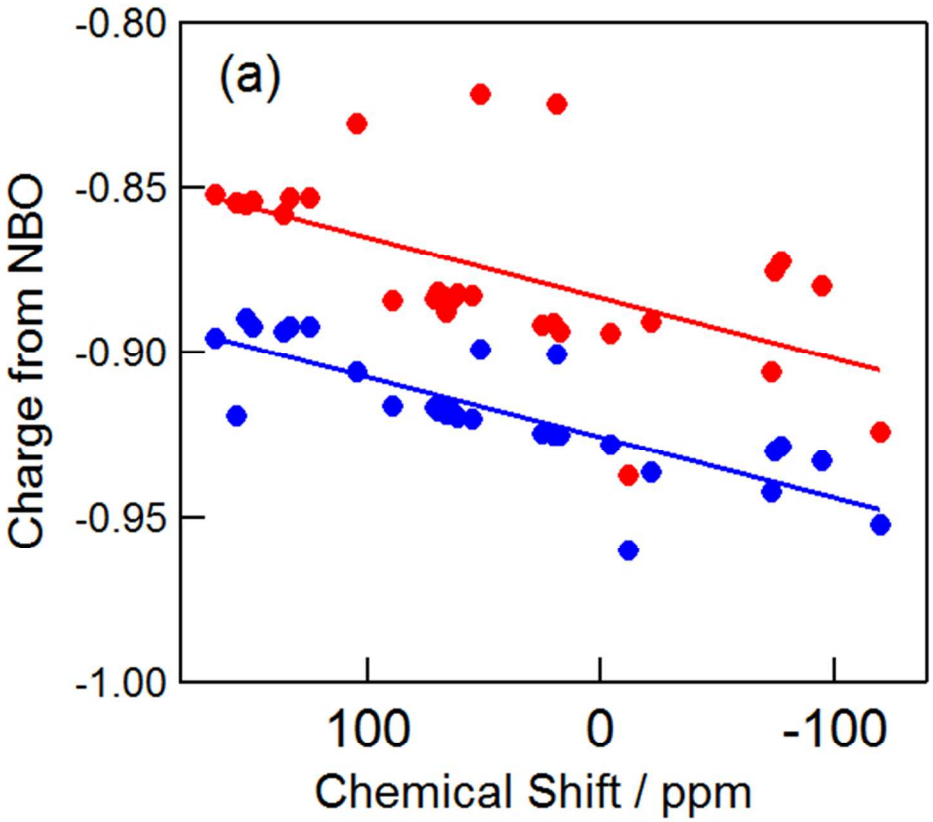

104x91mm (150 x 150 DPI)

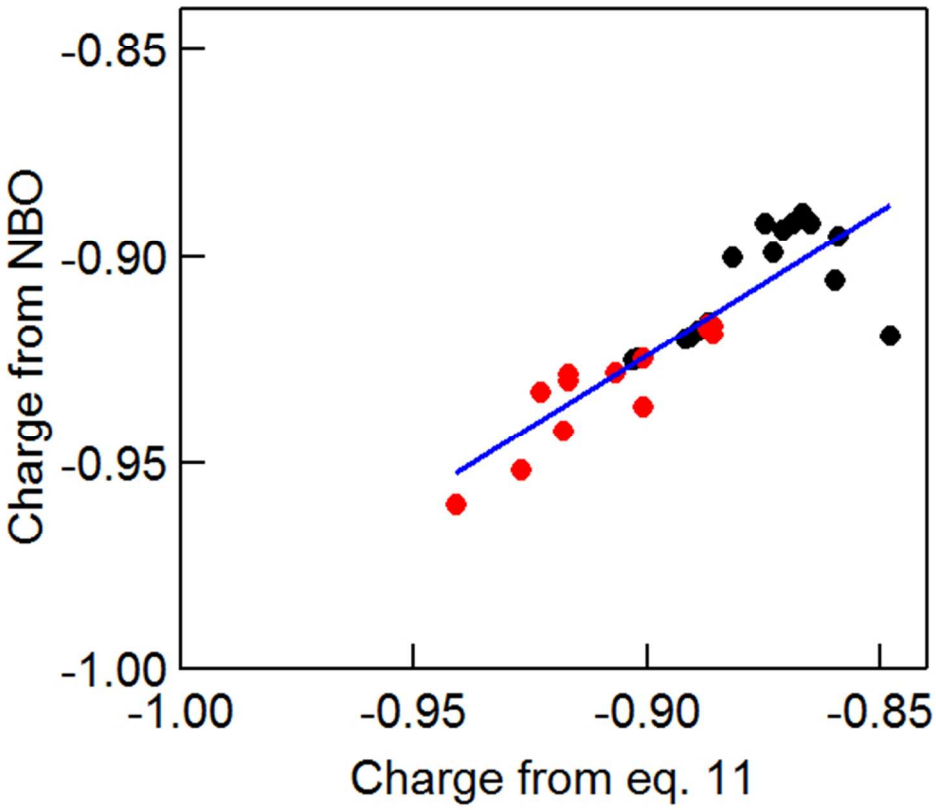

104x91mm (150 x 150 DPI)

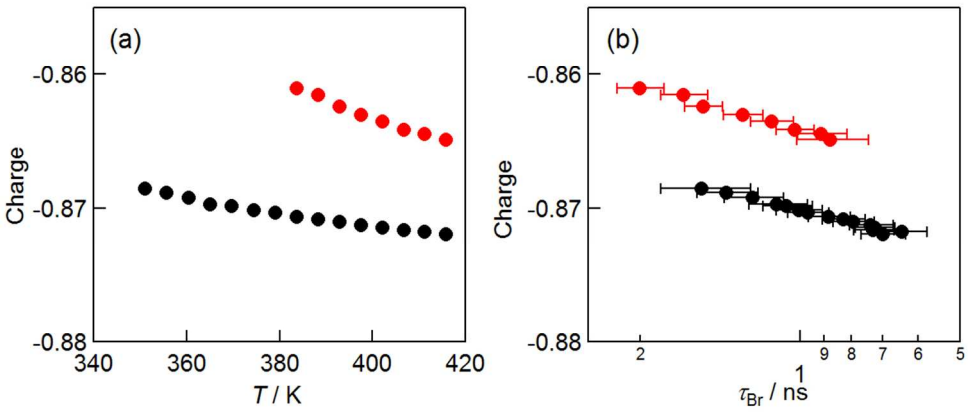

205x91mm (150 x 150 DPI)